A Boost DC–AC Converter: Analysis, Design, and Experimentation

Ramón O. Cáceres, *Member, IEEE,* and Ivo Barbi, *Senior Member, IEEE*

***Abstract*—This paper proposes a new voltage source inverter (VSI) referred to as a boost inverter or boost dc–ac converter. The main attribute of the new inverter topology is the fact that it generates an ac output voltage larger than the dc input one, depending on the instantaneous duty cycle. This property is not found in the classical VSI, which produces an ac output instantaneous voltage always lower than the dc input one. For the purpose of optimizing the boost inverter dynamics, while ensuring correct operation in any working condition, a sliding mode controller is proposed. The main advantage of the sliding mode control over the classical control schemes is its robustness for plant parameter variations, which leads to invariant dynamics and steady-state response in the ideal case. Operation, analysis, control strategy, and experimental results are included in this paper. The new inverter is intended to be used in uninterruptible power supply (UPS) and ac driver systems design whenever an ac voltage larger than the dc link voltage is needed, with no need of a second power conversion stage.**

***Index Terms*—Boost inverter, inverter, sliding mode control.**

I. Introduction

THE CONVENTIONAL voltage source inverter (VSI) shown in Fig. 1, referred to as a buck inverter in this paper, is probably the most important power converter topology. It is used in many distinct industrial and commercial applications. Among these applications, uninterruptible power supply (UPS) and ac motor drives are the most important. One of the characteristics of the buck inverter is that the instantaneous average output voltage is always lower that the input dc voltage.

As a consequence, when an output voltage larger than the input one is needed, a boost dc–dc converter must be used between the dc source and inverter as shown in Fig. 2.

Depending on the power and voltage levels involved, this solution can result in high volume, weight, cost, and reduced efficiency.

In this paper, a new VSI is proposed, referred to as boost inverter, which naturally generates an output ac voltage lower or larger than the input dc voltage depending on the duty cycle [1]–[5]. Details on analysis, control, and experimentation are presented in the subsequent sections.

Manuscript received May 12, 1997; revised June 8, 1998. Recommended by Associate Editor, K. Ngo.

R. O. Cáceres is with the Faculty of Engineering Electronics and Communication Department, Universidad de los Andes, Mérida, Venezuela.

I. Barbi is with the Electrical Engineering Department, Power Electronics Institute (INEP), Federal University of Santa Catarina, 88040-970 Florianópolis, SC, Brazil.

Publisher Item Identifier S 0885-8993(99)00299-9.

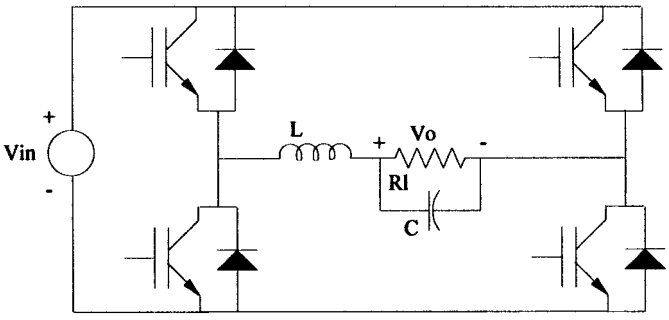

Fig. 1. The conventional VSI or buck inverter.

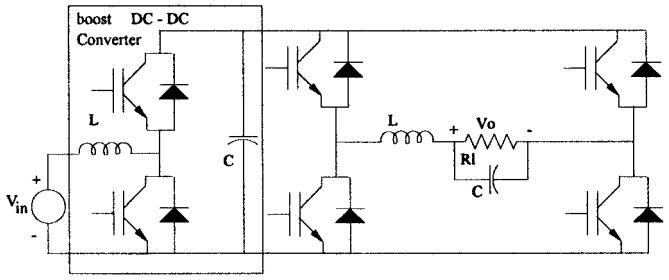

Fig. 2. Circuit used to generate an ac voltage larger than the dc input voltage.

II. The New Inverter and Principle of Operation

The proposed boost inverter achieves dc–ac conversion, as indicated in Fig. 3, by connecting the load differentially across two dc–dc converters and modulating the dc–dc converter output voltages sinusoidally. This concept has been discussed in [1] and [2], using the Cuk converter.

The blocks A and B represent dc–dc converters. These converters produce a dc-biased sine wave output, so that each source only produces a unipolar voltage. The modulation of each converter is 180° out of phase with the other, which maximizes the voltage excursion across the load. The load is connected differentially across the converters. Thus, whereas a dc bias appears at each end of the load, with respect to ground, the differential dc voltage across the load is zero. The generating bipolar voltage at output is solved by a push–pull arrangement. Thus, the dc–dc converters need to be current bidirectional.

The current bidirectional boost dc–dc converter is shown in Fig. 4. A circuit implementation of the boost dc–ac converter is shown in Fig. 5.

For a dc–dc boost converter, by using the averaging concept, we obtain the voltage relationship for the continuous

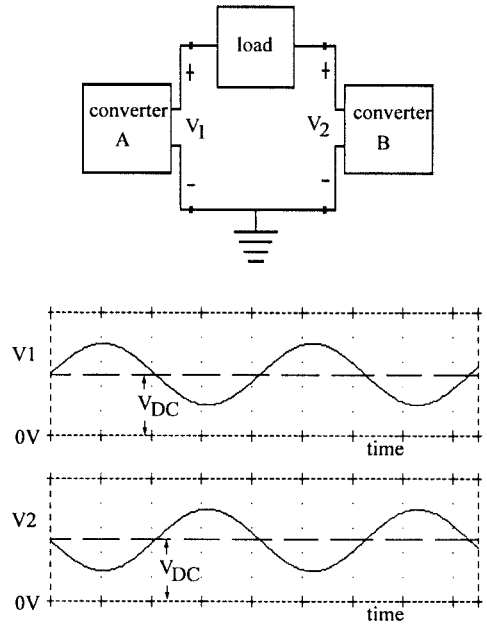

Fig. 3. A basic approach to achieve dc–ac conversion, with boost characteristics.

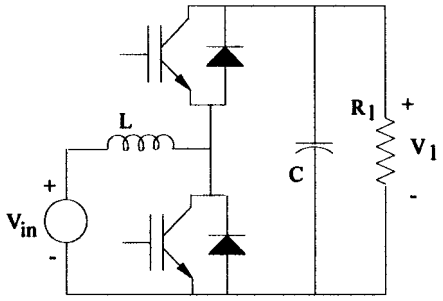

Fig. 4. The current bidirectional boost dc–dc converter.

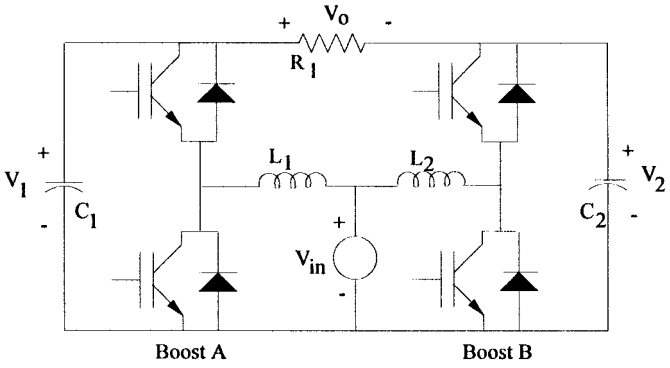

Fig. 5. The proposed dc–ac boost converter.

conduction mode given by

$$\frac{V_1}{V_{\text{in}}} = \frac{1}{1-D} \tag{1}$$

where D is the duty cycle.

The voltage gain, for the boost inverter, can be derived as follows: assuming that the two converters are 180° out of phase, then the output voltage is given by

$$V_0 = V_1 - V_2 = \frac{V_{\text{in}}}{1-D} - \frac{V_{\text{in}}}{D} \tag{2}$$

$$\frac{V_o}{V_{\text{in}}} = \frac{2D-1}{D(1-D)}. \tag{3}$$

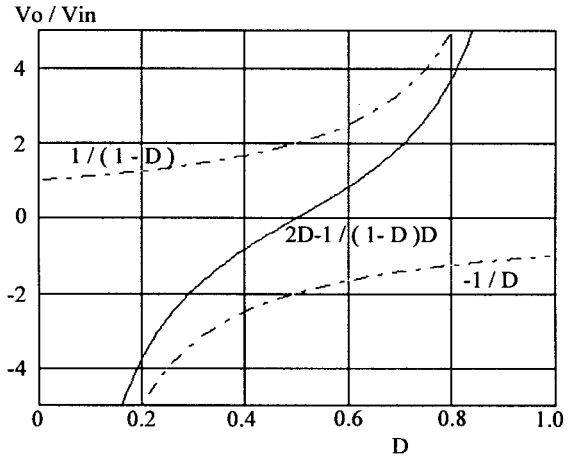

Fig. 6. DC gain characteristic.

The gain characteristic of the boost inverter is shown in Fig. 6. It is interesting to note that the feature of zero output voltage is obtained for $D = 0.5$. If the duty cycle is varied around this point, then there will be an ac voltage at the output terminal.

III. Sliding Mode Controller Analysis

For the purpose of optimizing the boost inverter dynamics, while ensuring correct operation in any working condition, a sliding mode controller is a more feasible approach.

Sliding mode control has been presented as a good alternative to the control of switching power converters [6]–[11]. The main advantage over the classical control schemes is its insusceptibility to plant parameter variations that leads to invariant dynamics and steady-state response in the ideal case. In this paper, a sliding mode controller for the boost inverter is proposed [10].

A. System Description

The boost dc–ac converter is shown in Fig. 7. It includes dc supply voltage V_{in}, input inductors L_1 and L_2, power switches S_1–S_4, transfer capacitors C_1 and C_2, free-wheeling diodes D_1–D_4, and load resistance R_1.

The principal purpose of the controllers A and B is to make the capacitor voltages V_1 and V_2 follow as faithfully as possible a sinusoidal reference.

The operation of the boost inverter is better understood through the current bidirectional boost dc–dc converter shown in Fig. 8.

In the description of the converter operation, we assume that all the components are ideal and that the converter operates in a continuous conduction mode. Fig. 9 shows two topological modes for a period of operation.

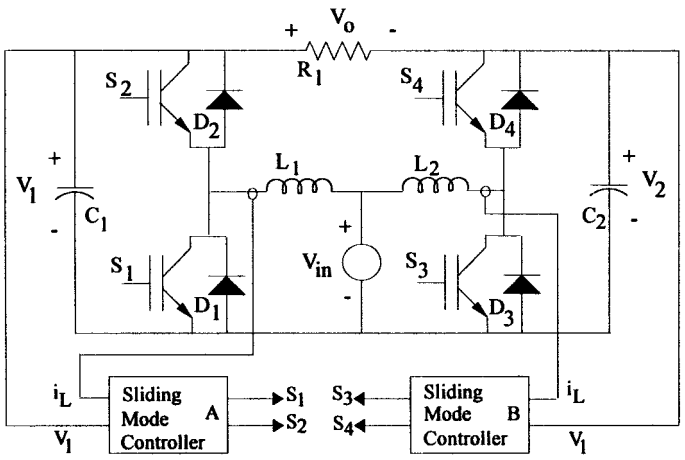

Fig. 7. The boost inverter controlled by sliding mode.

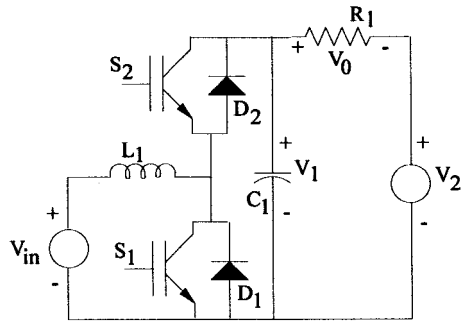

Fig. 8. Equivalent circuit for the boost inverter.

When the switch S_1 is closed and S_2 is open [Fig. 9(a)], current i_{L1} rises quite linearly, diode D_2 is reverse polarized, capacitor C_1 supplies energy to the output stage, and voltage V_1 decreases.

Once the switch S_1 is open and S_2 is closed [Fig. 9(b)], current i_{L1} flows through capacitor C_1 and the output stage. The current i_{L1} decreases while capacitor C_1 is recharged.

The state-space modeling of the equivalent circuit with state variables i_{L1} and V_1 is given by

$$\begin{bmatrix} \frac{di_{L1}}{dt} \\ \frac{dV_1}{dt} \end{bmatrix} = \begin{bmatrix} \frac{-R_a}{L_1} & \frac{-1}{L_1} \\ \frac{1}{C_1} & \frac{-1}{C_1 R_1} \end{bmatrix} \begin{bmatrix} i_{L1} \\ V_1 \end{bmatrix} + \begin{bmatrix} \frac{V_1}{L_1} \\ \frac{-i_{L1}}{C_1} \end{bmatrix} \gamma + \begin{bmatrix} \frac{V_{in}}{L_1} \\ \frac{V_2}{C_1 R_1} \end{bmatrix} \qquad \dot{v} = \mathbf{A}v + \mathbf{B}\gamma + \mathbf{C} \tag{4}$$

where γ is the status of the switches, v and $\dot{v}$ are the vectors of the state variables (i_{L1}, V_1) and their time derivatives, respectively,

$$\gamma = \begin{cases} 1 \rightarrow S_1\text{ON}, S_2\text{OFF} \\ 0 \rightarrow S_1\text{OFF}, S_2\text{ON}. \end{cases} \tag{5}$$

B. Sliding Mode Controller

When good transient response of the output voltage is needed, a sliding surface equation in the state space, expressed by a linear combination of state-variable errors ε_I (defined by difference to the references variables), can be given by [10]

$$S(i_{L1}, V_1) = K_1\varepsilon_1 + K_2\varepsilon_2 = 0 \tag{6}$$

where coefficients K_1 and K_2 are proper gains, ε_1 is the feedback current error, and ε_2 is the feedback voltage error, or

$$\varepsilon_1 = i_{L1} - i_{L\text{ref}} \tag{7}$$

$$\varepsilon_2 = V_1 - V_{\text{ref}}. \tag{8}$$

By substituting (7) and (8) in (6), one obtains

$$S(i_{L1}, V_1) = K_1(i_{L1} - i_{L\text{ref}}) + K_2(V_1 - V_{\text{ref}}). \tag{9}$$

The signal $S(i_{L1}, V_1)$, obtained by the hardware implementation of (9) and applied to a simple circuit (hysteresis comparator), can generate the pulses to supply the power semiconductor drives.

The corresponding control scheme is shown in Fig. 10. Status of the switch γ is controlled by hysteresis block H_1, which maintains the variable $S(i_{L1}, V_1)$ near zero.

The system response is determined by the circuit parameters and coefficients K_1 and K_2. With a proper selection of these coefficients in any operating condition, high control robustness, stability, and fast response can be achieved.

In theory, the sliding mode control requires sensing of all state variables and generation of suitable references for each of them. However, the inductor current reference is difficult to evaluate since that generally depends on load power demand, supply voltage, and load voltage. To overcome this problem, in practical implementation the state variable error for the inductor current $(i_{L1} - i_{L\text{ref}})$ can be obtained from feedback variable i_{L1} by means of a high-pass filter in the assumption that their low-frequency component is automatically adapted to actual converter operation. Thus, only the high-frequency component of this variable is needed for the control. This high-pass filter increases the system order and can heavily alter the converter dynamics. In order to avoid this problem, the cutoff frequency of the high-pass filter must be suitably lower than the switching frequency to pass the ripple at the switching frequency, but high enough to allow a fast converter response [10].

IV. Control Design Methodology

In the design of the converter, the following are assumed:

- ideal power switches;
- power supply free of sinusoidal ripple;
- converter operating at high-switching frequency.

A. Selection of Control Parameters

Once the boost inverter parameters are selected, inductances L_1 and L_2 are designed from specified input and output current ripples, capacitors C_1 and C_2 are designed so as to limit the output voltage ripple in the case of fast and large load variations, and maximum switching frequency is selected from

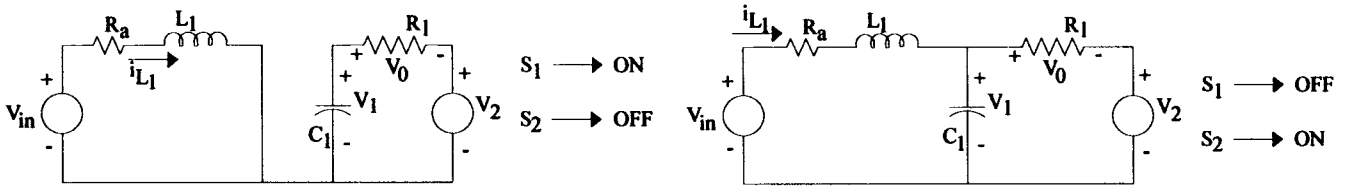

Fig. 9. Modes of operation.

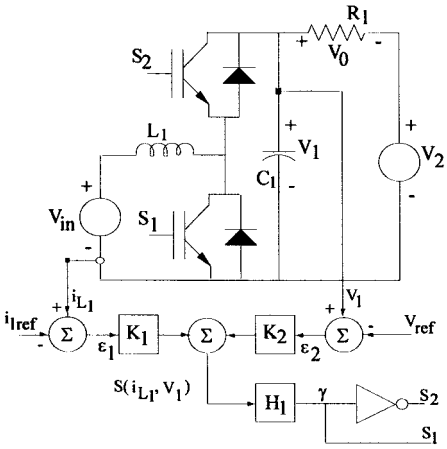

Fig. 10. Sliding mode controller scheme.

the converter ratings and switch type. The system behavior is completely determined by coefficients K_1 and K_2, which must be selected so as to satisfy existence and ensure stability and fast response, even for large supply and load variations.

According to the variable structure system theory, the converter equations must be written in the following form:

$$\dot{x} = \mathbf{A}x + \mathbf{B}\gamma + \mathbf{D} \tag{10}$$

where x represents the vector of state-variables errors, given by

$$x = v - V^* \tag{11}$$

where $V^* = [i_{L\text{ref}}, V_{\text{ref}}]^T$ is the vector of references.

By substituting (11) in (4), one obtains

$$\mathbf{D} = \mathbf{A}V^* + \mathbf{C} \tag{12}$$

$$\mathbf{D} = \begin{bmatrix} \dfrac{-R_a}{L_1} & \dfrac{-1}{L_1} \\ \dfrac{1}{C_1} & \dfrac{-1}{C_1R_1} \end{bmatrix} \begin{bmatrix} i_{L\text{ref}} \\ V_{\text{ref}} \end{bmatrix} + \begin{bmatrix} \dfrac{V_{\text{in}}}{L_1} \\ \dfrac{V_2}{C_1R_1} \end{bmatrix} \tag{13a}$$

$$\mathbf{D} = \begin{bmatrix} -\dfrac{V_{\text{ref}}}{L_1} + \dfrac{V_{\text{in}}}{L_1} - \dfrac{R_a i_{L\text{ref}}}{L_1} \\ -\dfrac{V_{\text{ref}}}{C_1R_1} + \dfrac{V_2}{C_1R_1} + \dfrac{i_{L\text{ref}}}{C_1} \end{bmatrix}. \tag{13b}$$

Substituting (11) in (9), the sliding function can be rewritten in the form

$$S(x) = K_1x_1 + K_2x_2 = K^Tx \tag{14}$$

where $K^T = [K_1,\ K_2]$ and $x = [x_1,\ x_2]^T$.

The existence condition of the sliding mode requires that all state trajectories near the surface are directed toward the sliding plane. The controller can enforce the system state to remain near the sliding plane by proper operation of the converter switches.

To make the system state move toward the switching surface, it is necessary and sufficient that [11]

$$\begin{cases} \dot{S}(x) < 0, & \text{if } S(x) > 0 \\ \dot{S}(x) > 0, & \text{if } S(x) < 0. \end{cases} \tag{15}$$

Sliding mode control is obtained by means of the following feedback control strategy, which relates to the status of the switches with the value of $S(x)$:

$$\gamma = \begin{cases} 0, & \text{for } S(x) > 0 \\ 1, & \text{for } S(x) < 0. \end{cases} \tag{16}$$

The existence condition (15) can be expressed in the form

$$\dot{S}(x) = K^T\mathbf{A}x + K^T\mathbf{D} < 0, \qquad S(x) > 0 \tag{17}$$

$$\dot{S}(x) = K^T\mathbf{A}x + K^T\mathbf{B} + K^T\mathbf{D} > 0, \qquad S(x) < 0. \tag{18}$$

From a practical point of view, assuming that error variables x_i are suitably smaller than references V^*, (17) and (18) can be rewritten in the form

$$K^T\mathbf{D} < 0, \qquad S(x) > 0 \tag{19}$$

$$K^T\mathbf{B} + K^T\mathbf{D} > 0, \qquad S(x) < 0. \tag{20}$$

By substituting matrices B and D in (19) and (20), one obtains

$$\frac{K_1}{L_1}[V_{\text{in}} - V_{\text{ref}} - R_a \cdot i_{L\text{ref}}] + \frac{K_2}{C_1R_1} \cdot [V_2 - V_{\text{ref}} + R_1 i_{L\text{ref}}] < 0 \tag{21}$$

$$\frac{K_1}{L_1}[V_{\text{in}} - R_a i_{L\text{ref}}] + \frac{K_2}{C_1R_1}[V_2 - V_{\text{ref}}] > 0. \tag{22}$$

The existence condition is satisfied if the inequalities (21) and (22) are true.

Finally, it is necessary to guarantee that the designed sliding plane is reached for all initial states. If the sliding mode exists, in the system defined by (10), it is a sufficient condition that coefficients K_1 and K_2 be nonnegative.

B. Switching Frequency

In the ideal sliding mode at infinite switching frequency, state trajectories are directed toward the sliding surface and move exactly along it. A practical system cannot switch at infinite frequency. Therefore, a typical control circuit features a practical relay, as indicated in Fig. 11.

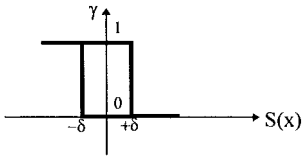

Fig. 11. Switching function γ.

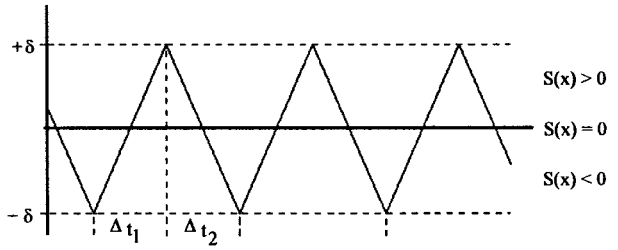

Fig. 12. The waveform of $S(x)$.

A practical relay always exhibits hysteresis modeled by

$$\gamma(s)=\begin{cases}0, & \text{when } S>+\delta \text{ or}\\ & \text{when } \dot{S}<0 \text{ and } |S|<\delta\\ 1, & \text{when } S<-\delta \text{ or}\\ & \text{when } \dot{S}>0 \text{ and } |S|<\delta\end{cases} \tag{23}$$

where δ is an arbitrarily small positive quantity and 2δ is the amount of hysteresis in $S(x)$. The hysteresis characteristic makes it impossible to switch the control on the surface $S(x)=0$. As a consequence, switching occurs on the lines $S=\pm\delta$, with a frequency depending on the slopes of i_{L1}. This hysteresis causes phase plane trajectory oscillations of width 2δ, around the surface $S(x)=0$, as shown in Fig. 12.

Note that Fig. 12 simply tells us that in Δt_1 function $S(x)$ must increase from $-\delta$ to $+\delta(\dot{S}>0)$, while in Δt_2 function $S(x)$ must decrease from $+\delta$ to $-\delta(\dot{S}<0)$.

The switching frequency equation is obtained from Fig. 12, by considering that the state trajectory is invariable, near to the sliding surface $S(x)=0$ and is given by

$$f_s=\frac{1}{\Delta t_1+\Delta t_2} \tag{24}$$

where Δt_1 is the conduction time of the switch S_1 and Δt_2 is the conduction time of the switch S_2. The conduction time Δt_1 is derived from (22) and it is given by

$$\Delta t_1=\frac{2\delta}{\dfrac{K_1}{L_1}\left[V_{\text{in}}-R_a i_{L\text{ref}}\right]+\dfrac{K_2}{C_1R_1}\left[V_2-V_{\text{ref}}\right]}. \tag{25}$$

The conduction time Δt_2 is derived from (21), and it is given by

$$\Delta t_2=\frac{-2\delta}{\dfrac{K_1}{L_1}\left[V_{\text{in}}-R_a i_{L\text{ref}}-V_{\text{ref}}\right]+\dfrac{K_2}{C_1R_1}\left[V_2+R_1 i_{L\text{ref}}-V_{\text{ref}}\right]}. \tag{26}$$

The maximum switching frequency is obtained substituting (25) and (26) in (24) in the assumption that the converter is operating with nonload ($i_{L\text{ref}}=0$ and $1/R_1=0$) and the output voltage reference is passing by maximum ($V_{\text{ref(max)}}$). It can be obtained using

$$f_{s(\max)}=\frac{K_1V_{\text{in}}}{2\delta L_1}\left(1-\frac{V_{\text{in}}}{V_{\text{ref(max)}}}\right). \tag{27}$$

C. Duty Cycle

The duty cycle $d(t)$ is defined by the ratio between the conduction time of the switch S_1 and the switch period time, as represented by

$$d(t)=\frac{\Delta t_1}{\Delta t_1+\Delta t_2}. \tag{28}$$

Considering the sliding mode control an instantaneous control, the ratio between the output and the input voltages must satisfy in any working condition

$$\frac{V_1(t)}{V_{\text{in}}}=\frac{1}{1-d(t)}. \tag{29}$$

D. Inductor Current i_{L1}

The inductor current is composed of two components. One of these is alternating with operation frequency. The other one is a high-frequency ripple caused by switching. In continuous-conduction mode, the maximum inductor current is obtained by using

$$i_{L1(\max)}=\frac{V_{\text{in}}-\sqrt{V_{\text{in}}^2-4R_a(-V_1(t))\left(\dfrac{V_2(t)-V_1(t)}{R_1}\right)}}{2R_a}. \tag{30}$$

The high-frequency ripple is obtained from Fig. 9(a) and given by

$$\Delta i_{L1}(t)=\frac{(V_{\text{in}}-R_a i_{L1}(t))\Delta t_1}{L_1}. \tag{31}$$

E. Voltage Capacitor V_1

The controller operates over the switch to make the voltage $V_1(t)$ follow a low-frequency sinusoidal reference. Over $V_1(t)$, a high-frequency ripple (switching) is imposed, which is given by

$$\Delta v_C(t)=\left|\frac{V_2(t)-V_1(t)}{C_1R_1}\right|\Delta t_1. \tag{32}$$

It is interesting to note that the switching frequency, inductor current ripple, and capacitor voltage ripple depend on the following: the control parameters, circuit parameters, reference voltage, output voltage of the other boost converter $V_2(t)$, and inductor current $i_{L1}(t)$.

It is important to determine the circuit parameters and coefficients K_1 and K_2 that agree with desirable values of maximum inductor current ripple, maximum capacitor voltage ripple, maximum switching frequency, stability, and fast response for any operating condition.

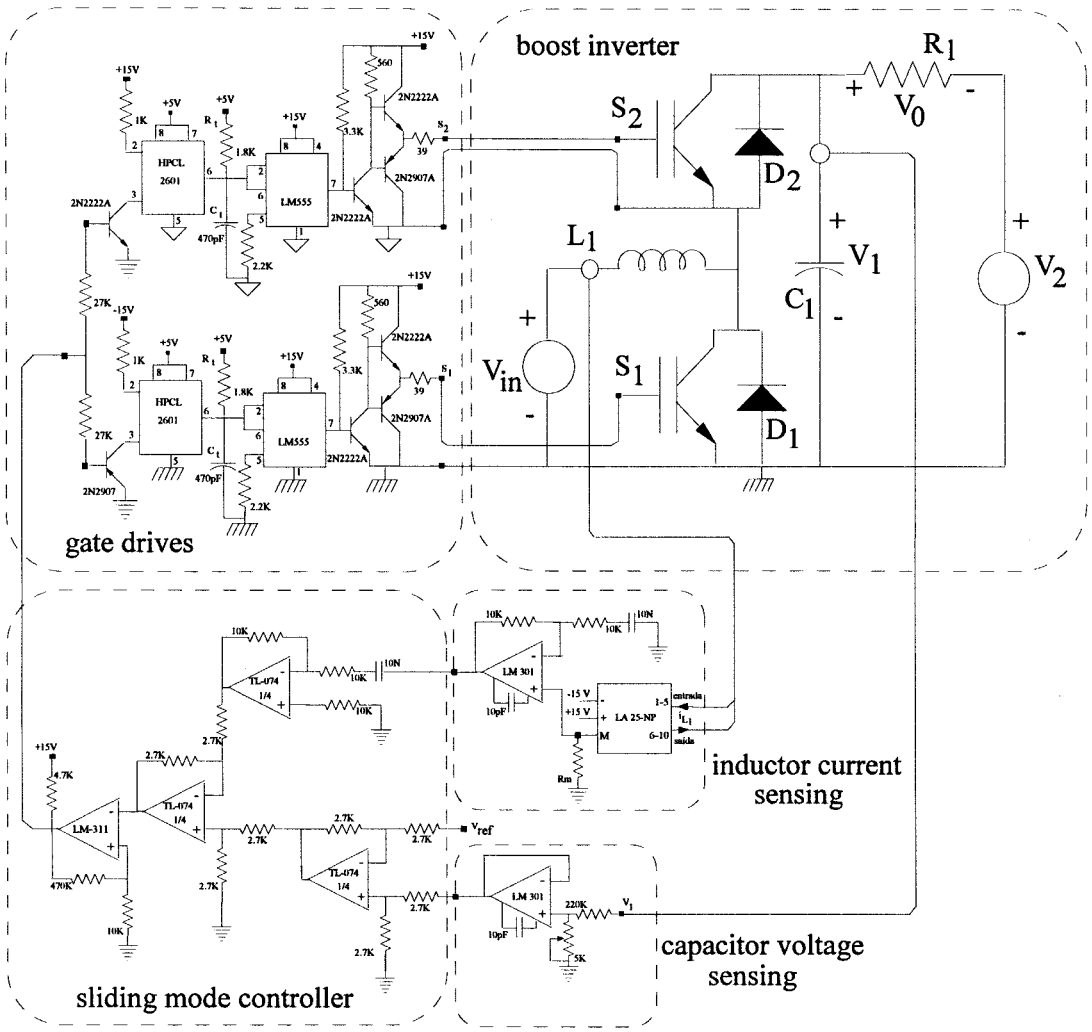

Fig. 13. Boost inverter scheme with sliding mode controller.

V. Design Example

The main purpose of this section is to use the previously deduced equations to calculate the prototype components value.

1) The Prototype Specifications:

P_0	500 W (output power);
V_0	127 Vrms (output voltage);
V_{in}	100 V (input voltage);
f_0	60 Hz (output voltage frequency);
$fs_{\max}$	30 kHz (maximum switching frequency).

2) Calculation of $V_1(t)$ and $V_2(t)$: In the boost inverter, the load voltage is determined by

$$V_0(t) = 180 S_{\text{in}}(377t) = V_1(t) - V_2(t).$$

Assuming that the two converters are 180° out of phase, the output voltages $V_1(t)$ and $V_2(t)$ are defined as

$$V_1(t) = V_{\text{dc}} + 90\,\text{Sin}(377t)$$
$$V_2(t) = V_{\text{dc}} - 90\,\text{Sin}(377t).$$

From (29) and a practical point of view, the V_{dc} value is chosen to produce a symmetrical variation of the duty cycle close to $D = 0.5$. The adopted value of the V_{dc} is 235 V, and a variation of the duty cycle between $D_{\min} = 0.3$ and $D_{\max} = 0.7$ is expected. Finally, the voltages $V_1(t)$ and $V_2(t)$ are given by

$$V_1(t) = 235 + 90\,\text{Sin}(377t)$$
$$V_2(t) = 235 - 90\,\text{Sin}(377t)$$

where $V_{1\max} = 325$ V.

3) Determining the Ratio K_1/L_1: Substituting V_{in}, $fs_{\max}$, $V_{\text{ref(max)}} = V_{1\max}$, and $\delta = 0.3$ in (27), one obtains

$$K_1/L_1 = 260.$$

4) Determining the Ratio K_2/C_1: From (21) and (22) and taking $i_{L\text{ref}} = i_{L1(\max)}$ (critical case), one obtains

$$0 < K_2/C_1 < 4200.$$

There are some degrees of freedom in choosing the ratio K_2/C_1. In this controller, the ratio K_2/C_1 is a tuning parameter. It is recommendable to choose the ratio K_2/C_1 to agree with proper values of stability and fast response.

In this work, the performance characteristics of the controller are specified in terms of the transient response to a

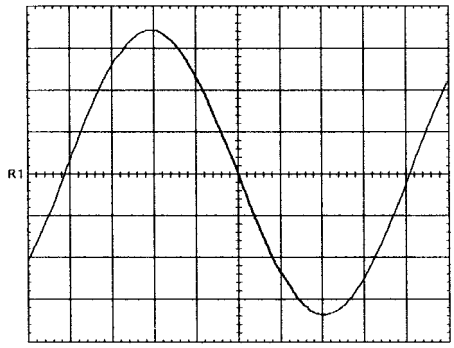

Fig. 14. Output voltage, nonload (50 V/div–2 ms/div).

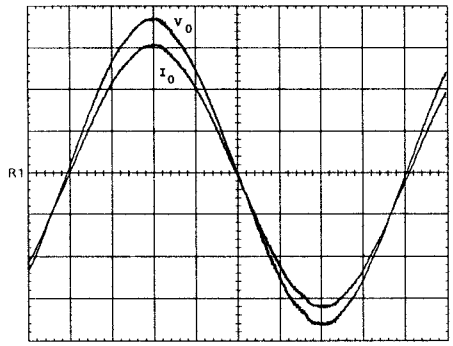

Fig. 15. Resistive load operation (50 V/div–2A/div–2 ms/div).

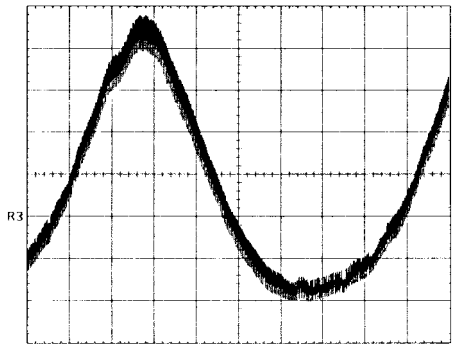

Fig. 16. Current through the inductor L_1 (5 A/div–2 ms/div).

unit-step input. It is specified the maximum overshoot that directly indicates the relative stability of the system and the settling time that is related to the largest time constant of the control system. It is desirable that the transient response be sufficiently fast and be sufficiently damped. The ratio K_2/C_1 was chosen by iterative procedure (this means that the ratio K_2/C_1 must be modified until the transient response is satisfactory), and it was verified by simulation.

Thus, the adopted value is

$$K_2/C_1 = 1000.$$

5) Calculation of L_1: The maximum inductor current ripple $\Delta i_{L1\,\max}$ is chosen to be equal to 20% of maximum inductor current, which one is obtained from (30). Then, from (31), substituting $i_{L1}(t) = i_{L1\,\max}$, one obtains $L_1 > 753\ \mu$H. $L_1 = 800\ \mu$H is adopted.

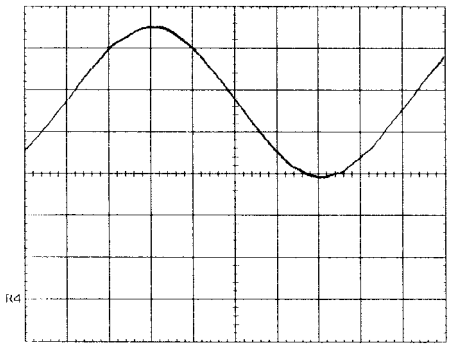

Fig. 17. Voltage across the capacitor C_1 (50 V/div–2 ms/div).

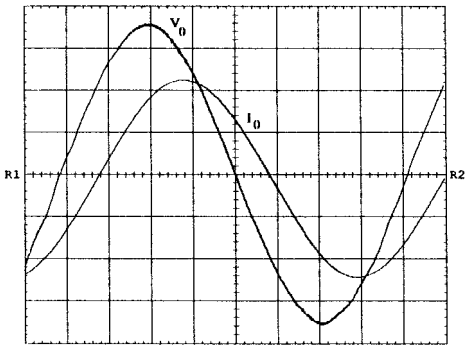

Fig. 18. Inductive load operation (50 V/div–2 A/div–2 ms/div).

6) Calculation of C_1: The maximum capacitor voltage ripple $\Delta Vc_{\max}$ is chosen to be equal to 5% of the maximum sinusoidal capacitor voltage. Then, from (31), one obtains $C_1 > 37.5\ \mu$F. $C_1 = 40\ \mu$F is adopted.

7) Values of the Coefficients K_1 and K_2: With the ratio K_1/L_1 and the value of inductor L_1, one obtains $K_1 = 0.208$.

With ratio K_2/C_1 and the value of capacitor C_1, one obtains $K_2 = 0.040$.

VI. Experimental Results

In order to confirm the effective performance of the boost inverter, a laboratory prototype was implemented (circuits are shown in Fig. 13), where V_2 is a boost converter.

The parameters of the circuit are as follows:

S_1–S_4	IRGBC40U (IGBT);
D_1–D_4	MUR850 (diodes);
C_1, C_2	40 μF/600 V;
L_1, L_2	800 μH.

The parameters of the controller are: $K_1 = 0.208$, $K_2 = 0.040$, and $\delta = 0.3$ as calculated in the previous section.

The output voltage at nonload is shown in Fig. 14, with a total harmonic distortion (THD) equal to 0.8%.

Figs. 15–17 show experimental waveforms of the converter for a resistive load of 540 W, and $R_1 = 30\ \Omega$. The experimental results agree with those predicted theoretically. The output voltage THD is equal to 1.24%.

Fig. 18 shows experimental waveforms of the inverter output current and voltage for inductive load with $R_0 = 30\ \Omega$ and $L_0 = 50$ mH. The THD is 1.28%, and the third harmonic, which is the greatest value, is equal to 0.8%.

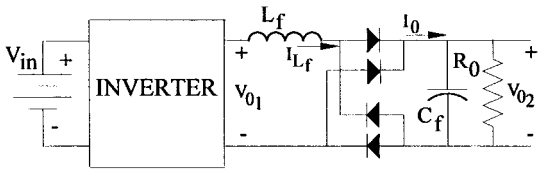

Fig. 19. Nonlinear load used with the boost inverter.

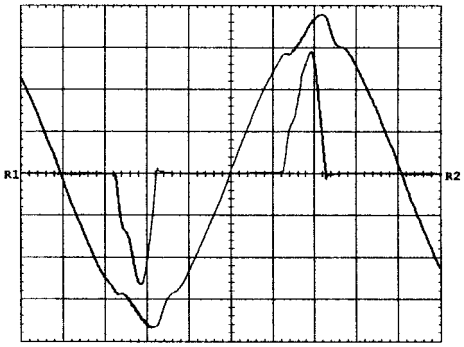

Fig. 20. Voltage V_{01} and current through the inductor L_f (50 V/div–2 A/div–2 ms/div).

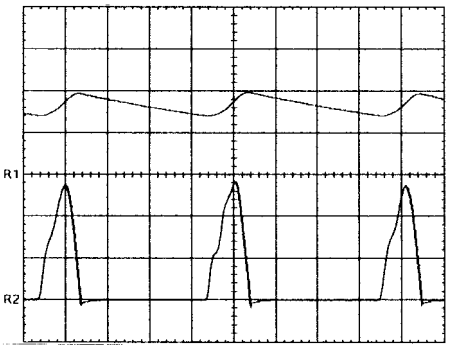

Fig. 21. Voltage and current in the nonlinear load (100 V/div–2 A/div–2 ms/div).

The boost inverter was also implemented with a nonlinear load, as is shown in Fig. 19. The component values are $R_0 = 170\ \Omega$, $C_f = 80\ \mu$F, and $L_f = 550$ mH.

Fig. 20 shows the inverter output voltage V_{01} and the current through the inductor L_f. The THD is 4.74%.

Fig. 21 shows the voltage and the current in the load. The average load voltage is 165 V, the average load current is 0.9 A, and the output power is 148.5 W.

VII. Conclusion

A dc–ac voltage source converter has been proposed and studied both theoretically and experimentally.

Due to the inherent nonlinearity, the sliding mode control has been employed to modulate and control the proposed converter, for linear and nonlinear loads, with converter experimental results in agreement with those predicted theoretically.

It is the authors' opinion that the boost inverter is suitable for applications where the output ac voltage needs to be larger than the dc input and can offer economic and technical advantages over the conventional VSI.

References

[1] F. Barzegar and S. Cuk, "Solid-state drives for induction motors: Early technology to current research," in *Proc. IEEE Region 6 Conf.,* Anaheim, CA, Feb. 15–18, 1982.

[2] ——, "A new switched-mode amplifier produces clean three-phase power," in *Proc. Powercon 9, 9th Int. Solid-State Power Electronics Conf.,* Washington, DC, July 13–15, 1982.

[3] R. Cáceres and I. Barbi, "A boost dc–ac converter: Operation, analysis, control and experimentation," in *Proc. Int. Conf. Industrial Electronics, Control and Instrumentation (IECON'95),* Nov. 1995, pp. 546–551.

[4] ——, "A boost dc–ac converter: Design, simulation and implementation," in *Proc. Power Electronic Brazilian Conf. (COBEP'95),* Dec. 1995, pp. 509–514.

[5] R. Cáceres, "DC–AC converters family, derived from the basic dc–dc converters," Ph.D. dissertation, Federal Univ. Santa Catarina, Brazil, 1997 (in Portuguese).

[6] H. Sira-Ramirez, "Sliding mode control of ac to ac converters," in *Proc. Brazilian Automatic Control Conf. (CBA'88),* pp. 452–457.

[7] M. Rios-Bolivar and H. Sira-Ramirez, "An extended linearization approach to sliding mode control of dc to dc power supplies," in *Proc. Power Electronic Brazilian Conf. (COBEP'91),* pp. 21–26.

[8] M. Carpita, P. Farina, and S. Tenconi, "A single-phase, sliding mode controlled inverter with three levels output voltage for UPS or power conditioning applications," in *Proc. European Power Electronic Conf. (EPE'93),* pp. 272–277.

[9] L. Malesani, L. Rossetto, G. Spiazzi, and P. Tenti, "Performance optimization of Cuk converter by sliding mode control," in *Proc. Applications Power Electronic Conf. (APEC'92),* pp. 395–402.

[10] ——, "General purpose sliding mode controller for dc–dc converter applications," in *Proc. Power Electronic Specialist Conf. (PESC'93),* pp. 609–615.

[11] H. Pinheiro, A. Martins, and J. Pinheiro, "Single-phase voltage inverters controlled by sliding mode," in *Proc. Brazilian Automatic Control Conf. (CBA'94),* pp. 1177–1182.

Ramón O. Cáceres (M'97) was born in San Cristóbal, Táchira, Venezuela, in 1959. He received the B.S. degree in electrical engineering from the Universidad de los Andes, Mérida, Venezuela, in 1983 and the M.S. and Ph.D. degrees from the Federal University of Santa Catarina, Florianópolis, Brazil, in 1993 and 1997, respectively.

In 1985, he joined the Department of Electronics, Universidad de los Andes, where he is currently an Associate Professor and a Member of the Power Electronics Research Group. His research interests include dc/dc and dc/ac converters, PF correction, and soft-switching techniques.

Ivo Barbi (M'78–SM'90), for a photograph and biography, see this issue, p. 97.